Published in final edited form as:
*Exp Biol Med (Maywood)*. 2009 February ; 234(2): 210–221. doi:10.3181/0807-RM-220.

# Monocyte Protein Signatures of Disease Severity in Sickle Cell Anemia

**Anita Hryniewicz-Jankowska**[*], **Pankaj K. Choudhary**[†], **Larry P. Ammann**[†], **Charles T. Quinn**[‡,§], and **Steven R. Goodman**[*,1,||]

[*]Department of Molecular & Cell Biology, University of Texas at Dallas, Richardson, Texas 75080

[†]Department of Mathematical Sciences, University of Texas at Dallas, Richardson, Texas 75080

[‡]Division of Hematology-Oncology, Department of Pediatrics, University of Texas Southwestern Medical Center, Dallas, Texas 75390

[§]Children's Medical Center Dallas, Dallas, Texas 75235

[||]Department of Cell Biology, University of Texas Southwestern Medical Center, Dallas, Texas 75390

## Abstract

Using two-dimensional difference gel electrophoresis (2D DIGE) we have analyzed monocytes derived from 10 sickle cell disease patients (5 males and 5 females ages 12–18) to generate hypotheses regarding signature proteins that appear most positively and negatively correlated with vasoocclusive event rate. Signature proteins have been identified by tandem mass spectrometry. Based on the limited number of samples analyzed, the most negatively correlated proteins related to crises rate were transketolase and coronin in the membrane fraction and heat shock 70 kDa protein cognate 4, and adenylate kinase isoenzyme 2, mitochondrial found in the cytosolic fraction. The protein spots that were most positively correlated with crisis rate in the cytoplasmic fraction were far upstream element-binding protein and Alpha actinin 1 or Alpha actinin 4. Utilizing StepSIM analysis, vinculin was able to classify all samples from the combined set and the membrane-only set, and cytosolic leukotriene A-4 hydrolase and phosphoglycerate kinase were also identified as important indicators for differentiating between low and high vasoocclusive event rates.

### Keywords

sickle cell disease; monocytes; 2D DIGE; tandem mass spectrometry; proteomics



[1]To whom correspondence should be addressed at SUNY Upstate Medical University, 750 East Adams Street, 1258 Weiskotten Hall, Syracuse, NY 13120. goodmans@upstate.edu.

## Introduction

Sickle cell anemia (SS) is a genetic disorder of red blood cells caused by a point mutation in the β-globin gene on chromosome 11 that replaces adenine with thymine, producing a single amino acid substitution of valine for glutamic acid in the sixth residue. Despite the same genetic defect in all homozygous SS patients, there is considerable phenotypic heterogeneity among individuals with identical alleles at the β-globin locus (1, 2). Some patients with SS have frequent vasoocclusive complications and die young, whereas others seem little affected by the disease and may have a normal lifespan. For example, the Cooperative Study of Sickle Cell Disease (CSSCD) reported in 1991 that 39% of subjects in the cohort had no painful crises during the follow-up period, but 1% had more than 6 episodes per year (3). Furthermore, the 5% of individuals who had between 3 and 10 episodes of pain per year accounted for 33% of all episodes of pain in this cohort (3). Similarly, only 11% of children with SS will suffer a clinically overt stroke and 7% will die by 18 years of age (4, 5).

The explanations for such phenotypic heterogeneity remain incomplete. It is important to understand this variation, because this knowledge would allow better definition and prediction of disease severity. An accurate assessment of each individual's disease severity is needed to formulate an appropriate therapeutic plan. There are widely disparate therapeutic options for SCD, including simple preventive measures, the drug hydroxyurea, chronic red blood cell transfusions, and stem cell transplantation. These therapies have substantially different risks, and they need to be carefully chosen for each individual to best balance the risks of treatment with the severity of disease. An understanding of the biological explanations for phenotypic variation in SCD would ultimately permit this therapeutic balance, plausibly allow early pre-morbid prediction of disease severity, and lead to new targeted, disease-modifying therapies.

The "pain rate", or number of vasoocclusive episodes per year, is a quantitative measure of clinical severity that correlates with early death in SS patients over the age of 20 (3). Indeed, a natural history study indicated an approximately 15-year difference in the average lifespan of those patients who experienced 1 or fewer crises per year versus patients experiencing 3 or greater crises per year. A subsequent study by Platt *et al.* (6) demonstrated an increased risk of early death in those sickle cell patients who experienced acute chest syndrome (ACS), as well as other complications like renal failure, seizures, steady state leukocytosis, and a low level of fetal hemoglobin. Accordingly, in searching for phenotypic modifiers that lead to variations in disease severity, a reasonable starting point is to identify proteins that contribute to the frequency of vasoocclusive events, such as acute painful episodes and ACS.

The process of vasoocclusion has been separated into the following steps: endothelial activation, recruitment of adherent leukocytes, interactions of sickle erythrocytes with adherent leukocytes (also direct adhesion of sickle cells to the activated and damaged endothelium), and vascular clogging by heterotypic cell-cell aggregates (including the dense non-deformable irreversible sickle cells (ISC)) (7). Perelman *et al.* (8) have demonstrated that increased erythropoietic stress in sickle cell anemia patients, resulting in increased erythropoietin levels, leads to increased production of placenta growth factor (PIGF) by

CD34+ erythroid progenitor cells. PIGF is an angiogenic growth factor belonging to the vascular endothelial growth factor (VEGF) family. Circulating PIGF levels correlated with sickle cell severity and stimulated monocyte chemotaxis. Increased PIGF causes monocytes to increase their expression of proinflammatory cytokines (interleukin (IL)-1β, IL-8, and monocyte chemoattractant protein-1 (MCP-1) and tumor necrosis factor-α (TNF-α)). Monocytes are the mononuclear cells responsible for activating endothelial cells (9). Sickle Cell monocytes trigger nuclear factor (NF)-κβ nuclear translocation in endothelial cells and produce more IL-1β and TNF-α than normal monocytes. The result is increased expression of adhesion molecules including P-and E-selectins on the surface of activated endothelial cells. The adhesion of monocytes to the vascular endothelium is triggered by MCP-1 and IL-8 (10). Sickle red blood cells associate with leukocytes in SS mouse inflamed venules and the leukocytes associate with the venule endothelium as long as P- and E-selectins are being expressed (11). Thus one mechanism by which sickled red blood cells (RBCs) become attached to the vessel endothelium is through leukocyte attachment. But sickle cells also attach directly to the activated SS endothelium (12, 13). Low density reversibly sickled cells (RSCs) are more adherent than high density ISCs. Furthermore, Hebbel *et al.* (12) demonstrated that vasoocclusive severity correlated with *in vitro* SS RBC adhesivity. It is the low density reticulocytes and RSCs that adhere to the endothelial wall (13) and to leukocytes (11). Finally, the non-deformable ISCs become entrapped in the decreased lumen of the venule.

Several studies have implicated leukocyte counts in the phenotypic severity of SS. Leukocytosis is associated with the development of overt stroke (14), susceptibility to acute chest syndrome (15), occurrence of silent cerebral infarction (16), survival of SS patients (6), and prediction of future severe sickle cell disease (17). Monocytes are activated in SS and are thought to enhance vasoocclusion by activating the blood vessel endothelial wall (9).

In this study we determine whether alterations in the monocyte protein profile can be utilized as a predictor of clinical variation in SS severity as quantified by 5-year pain rate. As was mentioned above, we are expecting to see monocyte proteins that are the most positively and negatively correlated with severity as measured by vaso-occlusive event rate in sickle cell patients. We are using the proteomic tools of mass spectrometry coupled to multivariate statistical tools to identify monocyte signature proteins that are predictive of variation in clinical severity in SS. Since we only have a limited number of samples ($n$ = 10) available, our main aim here is to use the extensive data generated from these samples to develop hypotheses regarding proteins that are predictive of clinical severity. These hypotheses would need to be subsequently tested on a large sample.

## Materials and Methods

### Patients

After informed consent, blood samples were collected from 10 children (5 female and 5 male) with homozygous SS disease. All subjects were diagnosed with SS at birth by newborn screening for hemoglobinopathies and followed thereafter in the Pediatric Sickle Cell Program at Children's Medical Center Dallas. All patients in this program are tracked

prospectively in a comprehensive clinical database. Patients had to be at least 10 years of age to allow a minimum time for disease severity to become apparent.

We studied here a common, easily quantifiable manifestation of disease severity: the rate of acute vaso-occlusive (painful) events, which is prognostic of short-term and late adverse outcomes, such as pain and death (6, 18). We chose to study this single manifestation of disease severity, vasoocclusive (painful) events, rather than a heterogeneous, composite measure that comprised a number of different unrelated outcomes, such as pain, stroke, or ACS, because the pathophysiology of each complication is different. Accordingly, monocyte protein signatures of disease severity would likely differ based on the complication. Moreover, we could not study several other manifestations of disease severity, like renal failure and seizures, because these are infrequent in children with SS.

To ensure that each patient had the same duration of follow-up (because older patients will have more lifetime events), we analyzed only the number of vasoocclusive events in the 5 years preceding study entry. The vaso-occlusive event rate includes hospitalizations for acute vasoocclusive (painful) events in this 5-year interval. The sample of patients for this study was specifically selected to represent the wide range of vasoocclusive event rates (from very low to very high) in the Dallas Newborn Cohort (5). We also collected the steady-state hematologic parameters of patients, such as steady-state hemoglobin concentration, reticulocyte count, and leukocyte count as well as the proportion of fetal hemoglobin.

## Sample Preparation

Peripheral whole blood was collected in Vacutainer tubes containing $K_3$EDTA, sufficient for 10 ml of blood, and processed immediately after collection. The RBCs were sedimented at 550 × *g* for 20 minutes at 20°C. Plasma was discarded and the RBC pellet and buffy coat diluted four times in 1X Dulbecco's Phosphate-Buffered Saline without calcium chloride and magnesium chloride (Gibco, Carlsbad, CA). Thirty five ml of diluted cell suspension was carefully layered over 15 ml Ficoll Paque (1.077 density, GE Healthcare, Piscataway, NJ) and centrifuged at 400 × *g* for 30 minutes at 20°C without brake. The mononuclear cell layer at the interphase was carefully transferred to new conical tube and washed two times with phosphate-buffered saline (PBS) buffer. For removal of platelets, the cell pellet was resuspended in PBS and centrifuged at 200 × *g* for 15 minutes at 20°C. Most of the platelets remain in the supernatant upon centrifugation at 200 × *g*. The cell pellet was resuspended in PBS buffer containing 2 mM EDTA and 0.5% BSA, cells were counted and then sorted by magnetic labeling.

## Magnetic Cell Sorting

The $CD14^+$ cells were magnetically labeled with CD14 MicroBeads utilizing a monocyte isolation kit from Miltenyi Biotech (Auburn, CA). The suspension was loaded on a column that was placed in the magnetic field of the magnetic cell sorting (MACS) separator. The magnetically labeled $CD14^+$ cells were retained on the column. The unlabeled cells ran through so the retained cell fraction was depleted of $CD14^+$ cells. After removal of the column from the magnetic field, the magnetically retained $CD14^+$ cells were eluted as the

positively selected cell fraction. Monocyte purity as well as activation level of isolated monocytes in each cell preparation were evaluated by flow cytometry analysis (FACSCalibur, San Jose, CA) using immunostaining for surface expression of $CD14^+$ and CD11b, respectively.

### Fractionation of Monocytes

Our method was a modification of that of Huber *et al.* (19). The cells were resuspended in buffer containing 250 mM sucrose; 3 mM imidazole, pH 7.4; 1 mM EDTA and tablet of protease inhibitors (Roche Diagnostic, Indianapolis, IN). The cells were homogenized with a Glas-Col motor homogenizer (Terre Haute, IN) on maximum speed (4000 rpm) on ice until the cell suspension became clear. The nuclei were pelleted at 800 × *g* for 10 minutes, 4°C, and supernatant was centrifuged at 100,000 × *g* at 4°C to obtain a pellet membrane fraction and a supernatant cytosolic fraction. Both pellets of nuclei and the membrane fraction were resuspended in extraction buffer containing: 20 mM N-(2-hydroxyethyl)-piperazine-N′-2-ethanesulfonic acid (HEPES), pH 7.0; 100 mM KCl; 1 mM DTT; 2 mM $MgCl_2$; 2% ASB-14 detergent and protease inhibitors tablet. Cytosolic and membrane fractions containing 150 μg and 200 μg, respectively, were purified by using a 2D Clean-up Kit (GE Healthcare, Piscataway, NJ) and freeze-dried pellets were stored at −80°C.

### Protein Labeling

Cytosolic and membrane proteins from ten different patients were solubilized in labeling buffer containing: 30 mM Tris-HCl, pH 8.5, 7 M urea, 2 M thiourea, and 2% ASB-14. All ten cytosolic and membrane fractions were assayed for total protein content and then equal amounts (50 μg) of all ten cytosolic protein fractions were pooled as a cytosolic internal standard and all ten membrane protein fractions as a membrane internal standard. Equal amounts of patient cytosolic proteins (50 μg) and membrane proteins (50 μg) were labeled with two different fluorophores (Cy3 and Cy5), according to the manufacturer's protocol (GE Healthcare, Piscataway, NJ). The same cytosolic and membrane internal standard sample (50 μg) was labeled with Cy2. Individual gels were then run with mixed equal amounts of total protein (50 μg) from the pooled cytosolic internal standard (Cy2) and two different individual cytosolic samples (each 50 μg) labeled with Cy3 and Cy5, respectively. The same scheme was performed for membrane proteins where the pooled membrane internal standard (50 μg) was labeled with Cy2 and mixed with two individual membrane fractions (50 μg) labeled with Cy3 and Cy5, respectively, and run on a 2D gel.

### 2D Gel Electrophoresis

Mixtures of labeled proteins were separated by 2D gel electrophoresis as we previously described (20). The first dimension, isoelectric focusing (IEF), was performed in 13-cm Immobiline DryStrip with a nonlinear pH 3–10 gradient using Ettan IPGphor II (GE Healthcare, Piscataway, NJ) at 20°C. Immobiline strip rehydration was performed for 12 hours in rehydration buffer (1% IPG buffer (GE Healthcare, Piscat-away, NJ), pH 3–10 NL; 7 M urea; 2 M thiourea; 2% ASB14; and 40 mM DTT) containing 150 μg of Cy2-, Cy3-and Cy5-labeled cytosolic or Cy2-, Cy3- and Cy5-labeled membrane proteins. Isoelectric focusing was performed in three steps: at 500 V for 1 hr, at 1000 V for 1 hr, and at 8000 V

for 33,300 Vhr. Prior to the second dimension, the Immobiline strip was equilibrated and reduced in a solution containing 50 mM Tris-HCl, pH 8.5, buffer, 2% SDS, 30% glycerol, and 5 mg/ml DTT at 90°C for 1 min. This was followed by equilibration and protein alkylation (carbami-domethylation) at room temperature in the Tris-HCl buffer containing 6 M urea, 2% SDS, 30% glycerol, and 20 mg/ml iodoacetamide for 10 min. After equilibration and alkylation the proteins separated by IEF were further separated by SDS-PAGE on a 10% polyacrylamide gel. The separation was performed in a Hoefer SE 600 unit (GE Healthcare) at 30 mA/gel constant current until the dye front migrated to the bottom of the gel. Where indicated, the gels were stained with Sypro Ruby (Molecular Probes, Eugene, OR) according to the manufacturer's protocol.

### Gel Image Analysis

The separated proteins labeled with Cy2, Cy3, and Cy5 fluorophores were detected in the 2D gels using a 2920 2D-Master Imager (GE Healthcare, Piscataway, NJ). After detection, the identical Cy2-, Cy3-, and Cy5-labeled proteins migrating to the same 2D spot were quantified based on the corresponding fluorescence intensities, and their molar ratios Cy3/Cy2 and Cy5/Cy2 were calculated using DeCyder Differential In-Gel Analysis software (GE Healthcare).

### Protein Identification

Selected 2D gel spots were analyzed for protein identification of corresponding tryptic peptides. The selected spots were excised from Sypro Ruby-stained 2D gel using an Ettan Spot Picker (GE Healthcare, Piscataway, NJ). Proteins in the excised gel pieces were digested using an in-gel trypsin digestion kit (Pierce, Rockford, IL), and corresponding tryptic digests were collected according to the manufacturer's protocol. Peptides in each tryptic digest were separated and identified by LC-MS/MS and database searching.

### Mass Spectrometry

The LC-MS/MS analysis was performed using a Surveyor high-performance liquid chromatography (HPLC) system connected through Pep-Finder kit (with peptide trap and 99:1 flow splitter) to a LCQ DECA XP ion trap mass spectrometer with a nanospray ionization source (ThermoFinnigan, San Jose, CA). Peptides in the tryptic digest (10 μl) were separated by reverse-phase HPLC on a PicoFrit BioBasic C18 column (New Objectives, 0.075 × 100 mm) at 0.3 μl/min flow rate. Water and acetonitrile with 0.1% formic acid each were used as solvents A and B, respectively. The gradient was started and kept for 10 min at 0% B, then ramped at 60% B in 60 min, finally ramped to 90% B for another 15 min. The eluted peptides were analyzed in data-dependent MS experiments ("big three") with dynamic exclusion as previously described (21). The spray voltage was set at 2.4 kV; the ion transfer capillary temperature was set at 180°C.

### Database Search

Raw mass spectra were converted to DTA peak list using BioWorks Browser 3.3 (Thermo-Finningan, San Jose, CA) with the following parameter settings: precursor mass ± 1.4 Da, total ion current (TIC) threshold $10^5$, group scan 15, minimum group count 1, and minimum

ion count 20. Each selected MS/MS spectrum was searched against the NCBI nonredundant protein sequence database (nr.fasta, February 15, 2007) containing 4,554,902 sequences using the SEQUEST software (22, 23) tool version 28 (rev. 12). The software creates theoretical peptides for all, or a limited group of, database proteins; calculates corresponding MS/MS spectra; and compares them to an experimental spectrum (submitted for the database search) to find the match. The database search was restricted to 700–3500 molecular mass tryptic peptides of human (*Homo sapiens*) origin (531,984 entries). Up to two missed trypsin cleavage sites were allowed and cysteines were considered carbamidomethylated. The acceptable molecular mass difference (mass tolerance) between an experimental and database peptides was set to 2.0 mass unit. Mass tolerance for experimental and calculated MS/MS fragment ions was set to 1. We used conservative criteria for peptide identification. The candidate database peptide with the highest Xcorr score was considered the match if the following identification criteria were met: 1) Xcorr of at least 2.0, 2.2 and 3.3 for singly, doubly, and triply charged peptides, respectively, 2) dCn of at least 0.1 regardless of charge state, and probability of 0.005 or less. The proteins were identified through a unique set of at least three tryptic peptides which meet the stated peptide identification criteria with protein probabilities of 0.001 or less. The protein sequences were examined using the BLAST tool to eliminate redundancy. A single-protein member of a multi-protein family, or set of isoforms, was identified if at least one identified tryptic peptide was present in that protein and was absent in the others. Also, a protein was identified only if its calculated molecular mass matched the apparent molecular mass (based on gel electrophoresis). If these two criteria were not met, all isoforms or potential sources of a set of detected tryptic peptides were listed.

## Statistical Analysis

**PPLS Regression Methodology for Identifying a Small Set of Proteins that Are Either Positively or Negatively Correlated with Severity—**Our approach is first to model the relationship between protein ratios and severity using a regression model. Then, we look at the signs of the regression coefficients to identify positively and negatively correlated proteins. In the regression model, the protein ratios serve as the predictors and the severity serves as the response. Note, however, that the ordinary least squares (OLS) regression cannot be used in this situation as the number of predictors ($p$) is very large and the sample size ($n$) is small. The partial least squares (PLS) regression is a viable alternative in this case. It is also becoming an important tool for analysis of genomic and proteomic data (24). The standard PLS analysis, however, gives a regression model relating *all* the proteins with severity. But we know beforehand that only a small subset of proteins would have strong enough relationship with severity to justify inclusion in the model—the others probably just contribute to the noise. The penalized PLS (PPLS) approach of Huang *et al.* (25) addresses this issue by shrinking some of the coefficients in the standard PLS model to zero, and thus eliminating the corresponding proteins from the model.

Let $X_{ij}$ be the ratio (on the natural log scale) associated with the $i$-th protein in the $j$-th patient, and $Y_j$ be the severity of the $j$-th patient; $i = 1, 2, \ldots, p$ and $j = 1, 2, \ldots, n$. Next, let $X_i$ be the $n$-dimensional column vector $(X_{i1}, \ldots, X_{in})^T$ and $\boldsymbol{Y}$ be the $n$-dimensional column vector $(Y_1, \ldots, Y_n)^T$.

Building a PPLS regression model using Huang *et al.* (25) that relates proteins to severity consists of the following steps:

1. Standardize each $X_i$ by subtracting its sample mean and dividing by its sample standard deviation.
2. Use leave-one-out cross validation to estimate the optimal values for the number of PLS components $q$ and the shrinkage parameter Δ. Let $T_1, \ldots, T_q$ denote the PLS components.
3. Fit the model $\hat{Y} = a_0 + a_1T_1 + \cdots + a_qT_q$ using OLS. Since each PLS component is a linear combination of $X_1, \ldots, X_p$, we can rewrite the model as $\hat{Y} = b_0 + b_1X_1 + \cdots + b_pX_p$.
4. Shrink the coefficients $b_1, \ldots, b_p$ by defining $\hat{b_i} = sign(b_i)((b_i) - \Delta)$ if $(b_i) > \Delta$, and $\hat{b_i} = 0$ if $(b_i) \leq \Delta$, $i = 1, \ldots, p$.
5. Define a new explanatory variable $T = \hat{b_1}X_1 + \cdots + \hat{b_p}X_p$ and fit the model $\hat{Y} = c_0 + c_1T$ using OLS. The last model is equivalent to

$$\hat{Y} = c_0 + c_1\hat{b}_1X_1 + \cdots + c_1\hat{b}_pX_p \quad (1)$$

The protein $i$ does not contribute to this model if $\hat{b_i} = 0$.

Using the model (1) built in step 5, the correlation between protein $i$ and severity is said to be positive if $c_1\hat{b_i} > 0$ and negative if $c_1\hat{b_i} < 0$. This methodology works well if only a small number of proteins have non-zero coefficients in model (1). When a large number of proteins contribute in model (1), we need to further rank them on the basis of their strength of correlation with severity. Frequently this ranking is of interest even when a small number of proteins are identified to be correlated with severity. The ranking is done by first estimating the standard errors (SE) of the coefficients in model (1) using jackknife (26) and standardizing the coefficients as $z_i = \hat{b_i}/\widehat{SE}(\hat{b_i})$, $i = 1, 2, \ldots, p$. These ratios are then sorted in decreasing order for the positively correlated proteins and in increasing order for the negatively correlated proteins. One can then select a small number of top ranked proteins in each group for further biological analysis.

In this study, our sample size (n) is only 10, but the number of proteins studied (p) is large: 445 for membrane fraction proteins and 426 for cytosolic proteins. Moreover, among the 10 patients in the sample, only 5 have non-zero crises rates. Hence, due to the limited number of samples available, the goal of this PPLS-based statistical analysis was to generate hypotheses regarding proteins that appear correlated with crisis rates. These hypotheses would need to be subsequently tested using a large $n$.

**Modified Version of the StepSIM Algorithm Toward Classification of Proteins that Are the Most Important Indicators for Differentiating Between Low and High Severity—**Protein ratios were converted to a signed log scale in which ratios greater than 1 (sickle cell protein abundance is greater than normal abundance) are transformed to the logarithm of the ratio and ratios less than 1 (sickle cell abundance is less than normal

abundance) are transformed to the negative of the logarithm of the ratios. That is, CL = sign(C)*log (abs(C)) where C is the original protein ratio, and sign(C) is the function that returns the value 1 if C > 0, 0 if C = 0, and −1 if C < 0. The severity measure was converted to a categorical variable by assigning to the Low category values of Severity ≤ 1 and assigning to the High category values of Severity > 1. This resulted in 6 samples assigned to the Low severity category and 4 samples assigned to the High severity category. A modified version of the StepSIM algorithm (27) was applied separately to the transformed Membrane and Cytosolic protein ratios. The version used here applied the variable selection component of StepSIM to all of the ratios in the respective sets. In addition, subsets of the membrane and cytosolic ratios were combined by selecting ratios within each group that remained in the stepwise model when 30% of the original ratios remained. This resulted in 133 cytosolic proteins and 134 membrane proteins in the combined set. StepSIM was then applied to this set of ratios. Just as in the case of the PPLS-based analysis, the results of this statistical analysis also would need to be validated using a large sample.

## Results

We analyzed changes in protein expression in the monocyte in relation to a quantitative and prognostic measure of disease severity, the 5-year vasoocclusive (painful) event rate, in well phenotyped SS patients using 2D DIGE (2 Dimensional Difference Gel Electrophoresis) technology. The clinical characteristics of the 10 patients are shown in Table 1. Our goal was to identify a small number of proteins that appear either positively or negatively correlated with severity and to determine which among them are the most important correlates of severity in SS patients. Peripheral blood monocytes were purified by gradient centrifugation followed by positive selection with specific monoclonal antibodies against CD14 coupled to para-magnetic beads. Flow cytometry analysis was used to assess the purity of the monocyte population which was >96% as well as to determine if isolated monocyte activation levels are similar in all analyzed blood samples. A well established marker of monocyte activation is CD11b, an α-chain integrin, expressed as a heterodimer complex with CD18, a β-chain integrin. The complex, also known as MAC-1, is translocated to the cell surface upon activation (28). It was apparent that most of the patient's monocytes are activated (mean 88.1% ± 3.5) before the isolation procedure in agreement with a previous study (9). After the isolation procedure expression of CD11b increased to 97% ± 1.02 ($P = 0.002$) as shown in Figure 1.

Monocytes were fractionated by homogenization and centrifugation into 100,000 × *g* supernatant (cytosolic) and 100,000 × *g* pellet (membrane) fractions. To determine the protein spots that are most positively and negatively correlated to crises rate, we labeled total cytosolic or membrane proteins from different patients with Cy3 and Cy5. An internal standard sample was labeled with Cy2 and run on each 2D gel. In ten experiments for cytosolic and membrane comparison, we observed over 500 fluorescent protein spots each. Spots for the 2D gel were quantified based on the corresponding fluorescence intensities, and their molar ratios Cy3/Cy2 and Cy5/Cy2 were calculated. All ratios were analyzed using statistical approaches, described below, to distinguish protein spots that appear either positively or negatively correlated with crisis rate. The PPLS methodology was used for this purpose.

First, we considered the membrane fraction proteins. The values of ($q$, Δ) in step 2 of the PPLS model building procedure were estimated as (1, 0.042). The final PPLS model in step 5 had 8 non-zero coefficients (1 positive and 7 negative). This resulted in 1 positively correlated protein spot and 7 negatively correlated protein spots.

In the case of the cytosolic proteins, ($q$, Δ) were estimated as (1, 0.031). Further, the final PPLS model had 64 non-zero coefficients (21 positive and 43 negative). Since this is clearly a large number of proteins, we ranked them further on the basis of their strength of relationship with severity, and selected the top 12 positively correlated proteins and the top 13 negatively correlated proteins. All 8 membrane and 25 cytosolic protein spots were analyzed by tandem mass spectrometry. Proteins were successfully identified in 5 out of 8 membrane spots (spot numbers: 764, 844, 847, 965 and 1442) and all of them are negatively correlated spots (Table 2). The plots of severity against log-ratios for these proteins are presented in Figure 2A. In the case of the cytosolic fraction 7 positively correlated proteins (spot numbers: 612, 485, 685, 57, 201, 913 and 749) and 9 negatively correlated proteins (spot numbers: 671, 1383, 997, 1111, 852, 791, 885, 799 and 802) were successfully identified (Tables 3, 4). The plots of severity versus log-ratio for these two sets of proteins are presented in Figures 2B and 2C. We note that several of the correlations exhibited in these graphs appear weak. This is especially true in case of cytosolic proteins. Moreover, in this case, the patient with 13 crises rate seems to be an outlier that magnifies the strengths of correlations. The position of the 5 membrane and 16 cytosolic identified protein spots is indicated on the two dimensional IEF SDS PAGE gels shown in Figure 3A and B, respectively.

The most negatively correlated proteins in the membrane fraction were transketolase identified in spots 844 and 847, coronin in spot 965, moesin in spot 764 and guanine nucleotide binding G protein present in spot 1442. In the cytosolic fraction the most positively correlated protein was far-upstream element-binding protein present in spot 612, alpha actinin 1 or alpha actinin 4 in spot 485, human serum albumin in a complex with myristic acid and tri-iodobenzoic acid in spot 685, filamin A in spot 57, integrin, alpha M in spot 201, Chain A, Apo form of human mitochondrial aldehyde dehydrogenase in spot 913 and less positive was leukotriene A-4 hydrolase present in spot 749.

The most negatively correlated protein was heat shock 70 kDa protein cognate 4 identified in spot 671 then adenylate kinase 2 variant AK2D in spot 1383, vimentin in spot 997, phosphoglycerate kinase 1 in spot 1111, protein disulfide-isomerase A3 in spot 852, t-complex protein 1 subunit alpha in spot 791, chaperonin containing TCP1, subunit 8 (Theta) in spot 799, adenylyl cyclase-associated protein in spot 885, and 60 kDa heat shock protein, mitochondrial [precursor] present in spot 802. Two of the identified proteins: adenylate kinase 2 variant and adenylyl cyclase-associated protein were detected by only two peptides. The Xcorr values for these peptides are high and experimental molecular masses and pI of the protein spots agree with the theoretical values for the identified proteins.

For one spot 485 that contains two isoforms of alpha actinin, we cannot be sure of the specific variation for an individual component.

Using the modified StepSIM algorithm (27), and selecting cytosolic protein spots 302, 749, and 1111 for the final cytosolic protein model, a leave-one-sample-out PLS classification based on these protein ratios was able to correctly classify the severity based on crisis rate for all samples. StepSIM selected membrane protein spots 490, 771, and 921 for the final membrane model and the leave-one-sample-out PLS classification. The ratios of these proteins were able to correctly classify the severity based on crisis rate for all samples. For the combined set of ratios for cytosolic and membrane spots, StepSIM selected for the final model membrane proteins 490, 759, and 771. This analysis predicts that Vinculin present in membrane spot 490 is the most important indicator for severity among all membrane and cytosolic spots. The proteins leukotriene A-4 hydrolase and phosphoglycerate kinase 1, identified in spots 749 and 1111, respectively, are also among the final 20 proteins selected by StepSIM from the combined set.

## Discussion

A major challenge of research in sickle cell disease is to understand the biological basis of the wide clinical variability among patients. In this study we identify monocyte protein expression signatures that correlate with the vasoocclusive event rate in well phenotyped children with SS who were followed from birth. We choose the vasoocclusive event rate because it is an easily quantified measure of disease severity that has been shown to be prognostic of early and late outcomes (6, 18).

Amongst membrane protein spots transketolase is the most negatively correlated to crises rate. This is a glycolytic enzyme involved in the pentose phosphate pathway. During serial analysis of comprehensive gene expression (SAGE) profile of LPS-stimulated human monocytes, more than 12,000 transcripts were sequenced. Among them trans-ketolase gene expression was decreased 11-fold compared to resting monocytes (29).

Dynamic reorganization of the actin cytoskeleton is a crucial component in nearly all aspects of cell motility and plays an important role in other processes such as host-pathogen interaction and endocytosis. The second most negatively correlated protein found in the membrane fraction was coronin, an f-actin binding protein which regulates a number of motility processes: migration, phagocytosis and chemotaxis (30). Since dynamic actin reorganization plays a significant role in leukocyte function, detailed study of the role of coronin in sickle monocytes should be pursued.

Monocyte cytosolic proteins that are most positively correlated with severity, as measured by vasoocclusive event rate, include far upstream element-binding protein (FBP). Duncan *et al.* demonstrated that the far upstream element-binding protein contains a transactivation domain which can function alone, suggesting that FBP contributes directly to c-*myc* transcription while bound to a single strand site. Furthermore, activation is mediated by a new motif which can be negatively regulated by a repression domain of FBP (31). Alpha actinin is a cross-linking protein which is thought to anchor actin to a variety of intracellular structures. Interaction of alpha actinin, vinculin and adhesion molecules such as integrins (all of them indicated in our results) in leukocytes is important in regulation of the initial adhesive interaction. A truncation mutant of L-selectin that lacks the 11 COOH-terminal

amino acid residues of the cytoplasmic domain has lost its ability to associate with cytoskeletal proteins alpha actinin and vinculin and was unable to support rolling on endothelium (32). Since adhesion of monocytes to blood vessel endothelial cells is a crucial aspect of vasoocclusion, these proteins are very important signatures for severity of sickle cell patients.

Heat shock 70 kDa protein cognate 4 had the strongest negative correlation among those negatively correlated with clinical severity. Other chaperones are also negatively correlated with severity (t-complex protein 1 subunit alpha, chaperonin containing TCP1, subunit 8 (theta), 60 kDa heat shock protein, mitochondrial [Precursor]). These proteins mediate the folding of newly translated polypeptides, and stabilize preexisting protein against aggregation. They also promote the refolding and proper assembly of unfolded polypeptides generated under stress conditions (33). During stress conditions, synthesis of chaperones is up-regulated. Similar results to ours were observed in patients with acute respiratory distress syndrome (ARDS) where HSP-70 inducibility was significantly reduced (34). In this study the authors suggested that HSP-70 expression level in peripheral blood monocytes of patients with ARDS would correlate with disease severity. The second most negatively correlated protein with clinical severity protein was mitochondrial adenylate kinase 2 (AK2). Recent studies have shown that mitochondrial adenylate kinase 2 mediates mitochondrial apoptosis through the formation of an AK2-FADD (Fas-associating protein with death domain)-cas-pase-10 (AFAC10) complex (35).

The StepSIM algorithm is designed to identify the smallest subset of proteins whose ratios can correctly classify the highest possible number of samples into their respective groups: subjects with high or low vasoocclusive rate. Among the cytosolic proteins, StepSIM identified spots 302, 749, and 1111 as the smallest such subset. Leukotriene A-4 hydrolase, one of the cytosolic proteins most positively correlated with crisis rate, was identified in spot 749. Phosphoglycerate kinase 1, one of the cytosolic proteins that was most negatively correlated with crisis rate, was identified in spot 1111. Since these proteins were identified by two different statistical methods, they are predicted to be important factors associated with the severity of sickle cell disease.

Leukotriene A-4 hydrolase hydrolyzes an epoxide moiety of leukotrienes A4 (LTA-4) to form leukotriene B4 (LTB-4) (36). Alternatively, LTA-4 may be conjugated with reduced glutathione (GSH), by specific S-transferase, to produce LTC-4. LTB-4 has been proposed to play a role in variety of acute and chronic inflammatory diseases and acts via specific seven-transmembrane, G protein-coupled surface receptors on the target cells (37). Montero *et al.* (38) studied regulation of leukotrienes A4 expression by different cytokines in peripheral monocytes. Interferon-gamma (a TH-2-derived cytokine) increased significantly LTA-4 hydrolase mRNA expression, whereas interleukin (IL)-4 and IL-13 (both TH-2-derived cytokines) decreased LTA-4 hydrolase mRNA expression in these cells. When LTB-4 release was measured, both IL-1 beta and interferon-gamma significantly increased LTB-4 production by monocytes, while TH-2 cytokines (IL-4 and IL-13) decreased it. The opposing effects of TH-1- and TH-2-derived cytokines on the expression of LTA-4 hydrolase mRNA may regulate LTB-4 synthesis by monocytes during inflammation.

Study of phosphoglycerate kinase 1 (PKG-1) in red blood cells revealed it to be a key enzyme for ATP generation in the glycolytic pathway (39). Inherited deficiency of PKG-1 is associated with chronic nonspherocytic hemolytic anemia and often with neurologic disorders (40). Administration of phosphoglycerate kinase to tumour-bearing mice caused an increase in plasma levels of angiostatin, and a decrease in tumour vascularity and rate of tumour growth. These findings indicate that phosphoglycerate kinase not only functions in glycolysis, but also is secreted by tumour cells and participates in the angiogenic process as a disulphide reductase (41).

Among membrane proteins, StepSIM identified spots 490, 759, and 771 as the smallest subset of proteins whose ratios can correctly identify all samples. Mass spectrometry revealed the spot 490 protein to be vinculin. In monocytes vinculin regulates adhesion and migration by providing a link between the actin-based microfilaments and trans-membrane receptors: integrins and cadherins. In addition to actin, vinculin interacts with other structural proteins such as talin and α-actinins (42). StepSIM was applied to the combined set of cytosolic and membrane proteins, and spot 490 also was identified as one of the important predictors of severity. These results show that vinculin is an important indicator for severity among monocyte proteins.

Two of the proteins predicted to be associated with sickle cell severity, vinculin (identified by StepSIM) and moesin (among the most negatively correlated with severity), also were shown to be two of the proteins with the greatest variation in the monocyte proteome of a general control population (43). There is no greater variance in the SS population than in the control AA populations for these two proteins.

The current study defines a class of monocyte proteins that is either positively or negatively correlated with phenotypic severity of SS, as measured by a vasoocclusive event rate. The most negatively correlated with severity were: transketolase, coronin, heat shock 70 kda protein cognate 4 and adenylate kinase 2 variant AK2D. The most positively correlated with severity were: far upstream element-binding protein and alpha actinin 1or alpha actinin 4. StepSIM analysis further predicts that vinculin, leukotriene a-4 hydrolase, and phosphoglycerate kinase 1 are important factors related to sickle cell disease severity. Our study might allow clinicians to utilize these proteins as laboratory signatures of clinical severity in SS, but we emphasize that these findings are based on the analysis of a limited number of samples. It is entirely possible that some of the associations discovered here are artifacts of chance, while others have been missed altogether. Thus, these findings need to be thoroughly validated using a large sample. In addition, an exploration of other measures of disease severity is also needed.

## Acknowledgments

This work was supported by a grant from the National Institutes of Health Sickle Cell Center (HL070588), which was awarded to Steven R. Goodman.

## References

1. Weatherall DJ. Phenotype-genotype relationships in monogenic disease: lessons from the thalassaemias. Nat Rev Genet. 2001; 2:245–255. [PubMed: 11283697]

2. Quinn CT, Miller ST. Risk factors and prediction of outcomes in children and adolescents who have sickle cell anemia. Hematol Oncol Clin North Am. 2004; 18:1339–1354. [PubMed: 15511619]
3. Platt OS, Thorington BD, Brambilla DJ, Milner PF, Rosse WF, Vichinsky E, Kinney TR. Pain in sickle cell disease: rates and risk factors. N Engl J Med. 1991; 325:11–16. [PubMed: 1710777]
4. Ohene-Frempong K, Weiner SJ, Sleeper LA, Miller ST, Embury S, Moohr JW, Wethers DL, Pegelow CH, Gill FM. Cerebrovascular accidents in sickle cell disease: rates and risk factors. Blood. 1998; 91:288–294. [PubMed: 9414296]
5. Quinn CT, Rogers ZR, Buchanan GR. Survival of children with sickle cell disease. Blood. 2004; 103:4023–4027. [PubMed: 14764527]
6. Platt OS, Brambilla DJ, Rosse WF, Milner PF, Castro O, Steinberg MH, Klug PP. Mortality in sickle cell disease. Life expectancy and risk factors for early death. N Engl J Med. 1994; 330:1639–1644. [PubMed: 7993409]
7. Frenette PS. Sickle cell vaso-occlusion: multistep and multicellular paradigm. Curr Opin Hematol. 2002; 9:101–106. [PubMed: 11844991]
8. Perelman N, Selvaraj SK, Batra S, Luck LR, Erdreich-Epstein A, Coates TD, Kalra VK, Malik P. Placenta growth factor activates monocytes and correlates with sickle cell disease severity. Blood. 2003; 102:1506–1514. [PubMed: 12714517]
9. Belcher JD, Marker PH, Weber JP, Hebbel RP, Vercolloti GM. Activated monocytes in sickle cell disease: potential role in activation of vascular endothelium and vaso-occlusion. Blood. 2000; 96:2451–2459. [PubMed: 11001897]
10. Gerszten RE, Garcia-Zepeda EA, Lim YC, Yoshida M, Ding HA, Gimbrone MA Jr, Luster AD, Luscinskas FW, Rosenzweig A. MCP-1 and IL-8 trigger firm adhesion of monocytes to vascular endothelium under flow conditions. Nature. 1999; 398:718–723. [PubMed: 10227295]
11. Turhan A, Weiss LA, Mohandas N, Coller BS, Frenette PS. Primary role for adherent leukocytes in sickle cell vascular occlusion: a new paradigm. Proc Natl Acad Sci U S A. 2002; 99:3047–3051. [PubMed: 11880644]
12. Hebbel RP, Boogaerts MA, Eaton JW, Steinberg MH. Erythrocyte adherence to endothelium in sickle cell anemia. A possible determinant of disease severity. N Engl J Med. 1980; 302:992–995. [PubMed: 7366623]
13. Hebbel RP. Adhesive interactions of sickle erythrocytes with endothelium. J Clin Invest. 1997; 99:2561–2564. [PubMed: 9169483]
14. Balkaran B, Char G, Morris JS, Thomas PW, Serjeant BE, Serjeant GR. Stroke in a cohort of patients with homozygous sickle cell disease. J Pediatr. 1992; 120:360–366. [PubMed: 1538280]
15. Castro O, Brambilla DJ, Thorington B, Reindorf CA, Scott RB, Gillette P, Vera JC, Levy PS. The acute chest syndrome in sickle cell disease: incidence and risk factors. The cooperative study of sickle cell disease. Blood. 1994; 84:643–649. [PubMed: 7517723]
16. Kinney TR, Sleeper LA, Wang WC, Zimmerman RA, Pegelow CH, Ohene-Frempong K, Wethers DL, Bello JA, Vichinsky EP, Moser FG, Gallagher DM, DeBaun MR, Platt OS, Miller ST. Silent cerebral infarcts in sickle cell anemia: a risk factor analysis. The cooperative study of sickle cell disease. J Pediatr. 1999; 103:640–645.
17. Miller ST, Macklin EA, Pegelow CH, Kinney TR, Sleeper LA, Bello JA, DeWitt LD, Gallagher DM, Guarini L, Moser FG, Ohene-Frempong K, Sanchez N, Vichinsky EP, Wang WC, Wethers DL, Younkin DP, Zimmerman RA, DeBaun MR. Silent infarction as a risk factor for overt stroke in children with sickle cell anemia. A report from the cooperative study of sickle cell disease. J Pediatr. 2001; 139:3985–3990.
18. Quinn CT, Shull EP, Ahmad N, Lee NJ, Rogers ZR, Buchanan GR. Prognostic significance of early vaso-occlusive complications in children with sickle cell anemia. Blood. 2007; 109:40–45. [PubMed: 16940426]
19. Huber LA, Pfaller K, Vietor I. Organelle proteomics: implications for subcellular fractionation in proteomics. Circ Res. 2003; 92:962–968. [PubMed: 12750306]
20. Kakhniashvili DG, Griko NB, Bulla LA Jr, Goodman SR. The proteomics of sickle cell disease: profiling of erythrocyte membrane proteins by 2D-DIGE and tandem mass spectrometry. Exp Biol Med (Maywood). 2005; 230:787–792. [PubMed: 16339742]

21. Kakhniashvili DG, Bulla LA Jr, Goodman SR. The human erythrocyte proteome: analysis by ion trap mass spectrometry. Mol Cell Proteomics. 2004; 3:501–509. [PubMed: 14963112]
22. Eng JK, McCormack AL, Yates JR 3rd. An approach to correlate tandem mass spectral data of peptides with amino acid sequence in a protein database. J Am Soc Mass Spectrom. 1994; 5:976–989. [PubMed: 24226387]
23. Yates JR 3rd, Eng JK, McCormac AL, Schieltz D. Method to correlate tandem mass spectra of modified peptides to amino acid sequence in the protein database. Anal Chem. 1995; 67:1426–1436. [PubMed: 7741214]
24. Nguyen DV, Rocke DM. Tumor classification by partial least squares using microarray gene expression data. Bioinformatics. 2002; 18:39–50. [PubMed: 11836210]
25. Huang X, Pan W, Park S, Han X, Miller L, Hall J. Modeling the relationship between LVAD support time and gene expression changes in the human heart by penalized partial least squares. Bioinformatics. 2004; 20:888–894. [PubMed: 14751963]
26. Westad F, Martens H. Variable selection in near infrared spectroscopy based on significance testing in partial least squares regression. J Near Infrared Spectrosc. 2000; 8:117–124.
27. Ammann LP, Merritt M. StepSIM: a method for stepwise peak selection and identification of metabolites in 1H NMR spectra. Metabolomics. 2007; 3:1–11.
28. Miller LJ, Bainton DF, Borregaard N, Springer TA. Stimulated mobilization of monocyte Mac-1 and p150,95 adhesion proteins from an intracellular vesicular compartment to the cell surface. J Clin Invest. 1987; 80:535–544. [PubMed: 3038962]
29. Suzuki T, Hashimoto S, Toyoda N, Nagai S, Yamazaki N, Dong HY, Sakai J, Yamashita T, Nukiwa T, Matsushima K. Comprehensive gene expression profile of LPS-stimulated human monocytes by SAGE. Blood. 2000; 96:2584–2591. [PubMed: 11001915]
30. Cai L, Makhov AM, Bear JE. F-actin binding is essential for coronin 1B function in vivo. J Cell Sci. 2007; 120:1779–1790. [PubMed: 17456547]
31. Duncan R, Collins I, Tomonaga T, Zhang T, Levens D. A unique transactivation sequence motif is found in the carboxyl-terminal domain of the single-strand-binding protein FBP. Mol Cell Biol. 1996; 16:2274–2282. [PubMed: 8628294]
32. Pavalko FM, LaRoche SM. Activation of human neutrophils induces an interaction between the integrin beta 2-subunit (CD18) and the actin binding protein alpha-actinin. J Immunol. 1993; 151:3795–3807. [PubMed: 8104223]
33. Young JC, Agashe VR, Siegers K, Hartl FU. Pathways of chaperone-mediated protein folding in the cytosol. Nat Rev Mol Cell Biol. 2004; 5:781–791. [PubMed: 15459659]
34. Durand P, Bachelet M, Brunet F, Richard MJ, Dhainaut JF, Dall'Ava J, Polla BS. Inducibility of the 70 kD heat shock protein in peripheral blood monocytes is decreased in human acute respiratory distress syndrome and recovers over time. Am J Respir Crit Care Med. 2000; 161:286–292. [PubMed: 10619833]
35. Lee HJ, Pyo JO, Oh Y, Kim HJ, Hong SH, Jeon YJ, Kim H, Cho DH, Woo HN, Song S, Nam JH, Kim HJ, Kim KS, Jung YK. AK2 activates a novel apoptotic pathway through formation of a complex with FADD and caspase-10. Nat Cell Biol. 2007; 9:1303–1310. (http://www.ncbi.nlm.nih.gov/pubmed/17952061?ordinalpos=2&itool=EntrezSystem2.PEntrez.Pubmed.Pubmed_ResultsPanel.Pubmed_RVDocSum). [PubMed: 17952061]
36. Haeggström JZ. Structure, function, and regulation of leukotriene A4 hydrolase. Am J Respir Crit Care Med. 2000; 161:25–31.
37. Yokomizo T, Izumi T, Chang K, Takuwa Y, Shimizu T. A G-protein-coupled receptor for leukotriene B4 that mediates chemotaxis. Nature. 1997; 387:620–624. [PubMed: 9177352]
38. Montero A, Nassar GM, Uda S, Munger KA, Badr KF. Reciprocal regulation of LTA(4) hydrolase expression in human monocytes by gamma-interferon and interleukins 4 and 13: potential relevance to leukotriene regulation in glomerular disease. Exp Nephrol. 2000; 8:258–265. [PubMed: 10940725]
39. Segel GB, Feig SA, Glader BE, Muller A, Dutcher P, Nathan DG. Energy metabolism in human erythrocytes: the role of phospho-glycerate kinase in cation transport. Blood. 1975; 46:271–278. [PubMed: 166715]

40. Huang IY, Fujii H, Yoshida A. Structure and function of normal and variant human phosphoglycerate kinase. Hemoglobin. 1980; 4:601–609. [PubMed: 7440217]

41. Lay AJ, Jiang XM, Kisker O, Flynn E, Underwood A, Condron R, Hogg PJ. Phosphoglycerate kinase acts in tumour angiogenesis as a disulphide reductase. Nature. 2000; 408:869–873. (http://www.ncbi.nlm.nih.gov/pubmed/11130727?ordinalpos=2&itool=EntrezSystem2.PEntrez.Pubmed.Pubmed_ResultsPanel.Pubmed_RVDocSum). [PubMed: 11130727]

42. Surin B, Rouillard D, Bauvois B. Interactions between human monocytes and fibronectin are suppressed by interferons beta and gamma, but not alpha: correlation with Rho-paxillin signaling. Int J Mol Med. 2002; 10:25–31. [PubMed: 12060847]

43. Hryniewicz-Jankowska A, Choudhary PK, Goodman SR. Variation in the monocyte proteome. Exp Biol Med (Maywood). 2007; 232:967–976. [PubMed: 17609514]

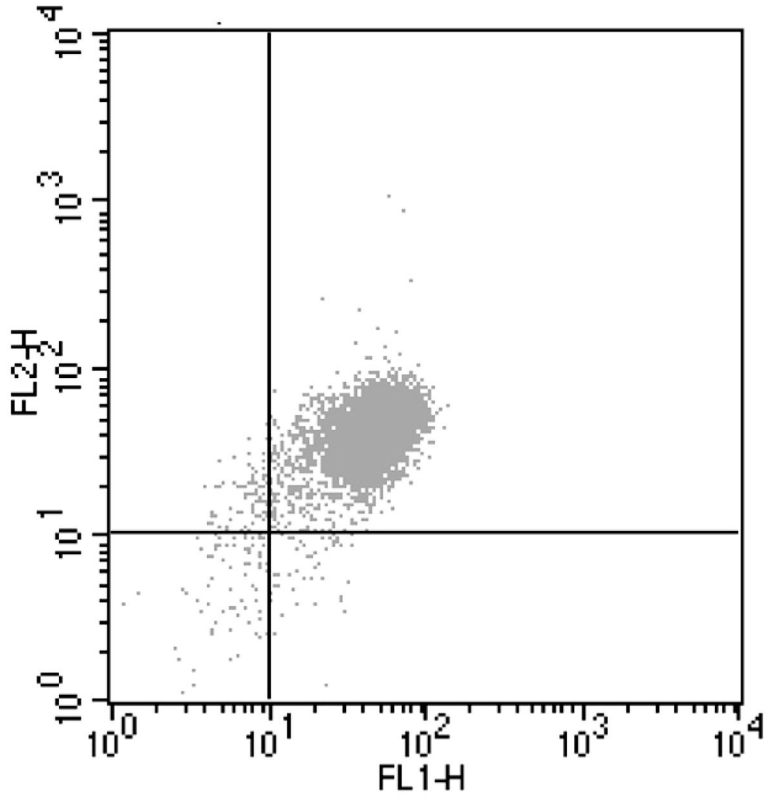


**Figure 1.**

Flow cytometric analysis of CD11b and CD14 expression on the surface of isolated monocytes from patient with sickle cell disease. A gate was placed around the mononuclear leukocytes based on their forward and side scatter. Monocytes within that gate were identified based on their expression of CD14-specific immuno-fluorescence. The crosshatch separates specific and nonspecific immunofluorescence. Cells to the right of the crosshatch are $CD14^+$ monocytes, and cells above the crosshatch are $CD11b^+$ monocytes. Monocytes in the upper right quadrant are activated and monocytes in the lower right quadrant are resting. In this example based on CD11b surface expression, 97% of the patient's isolated sickle monocytes are activated and 3% are resting.

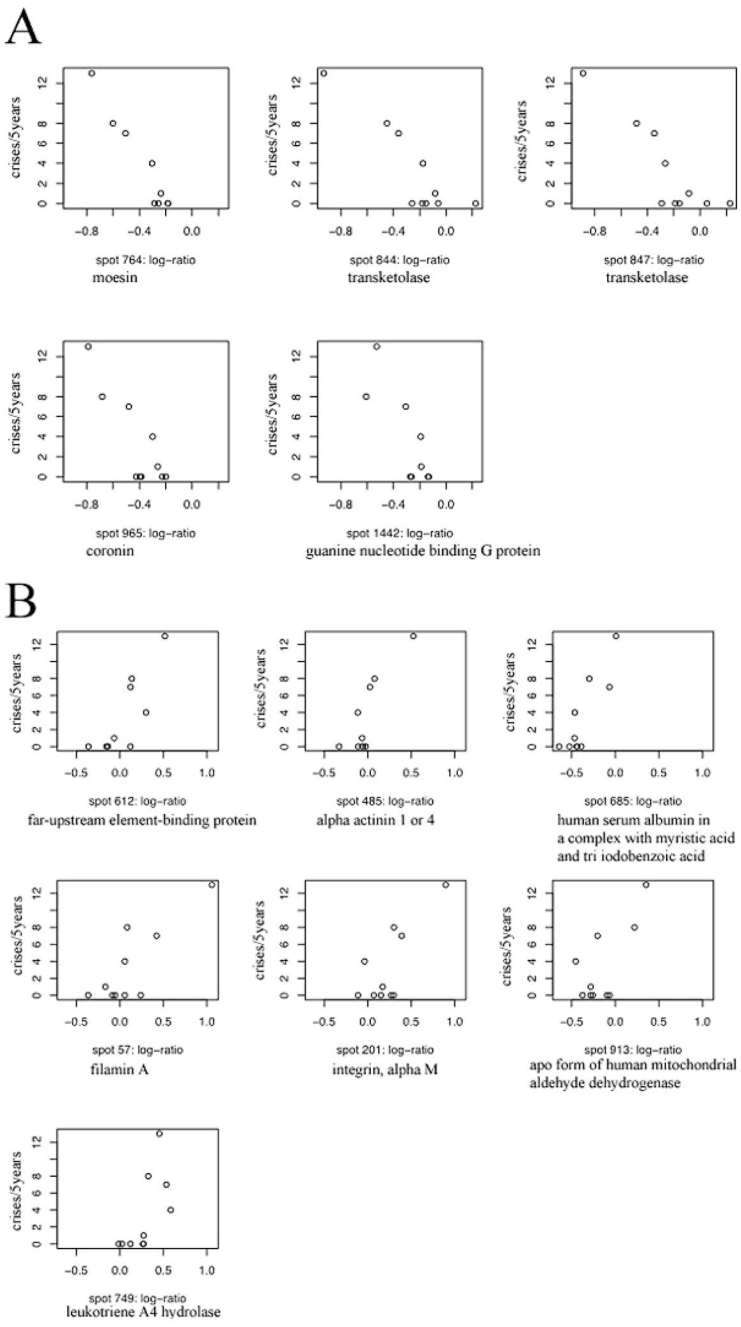

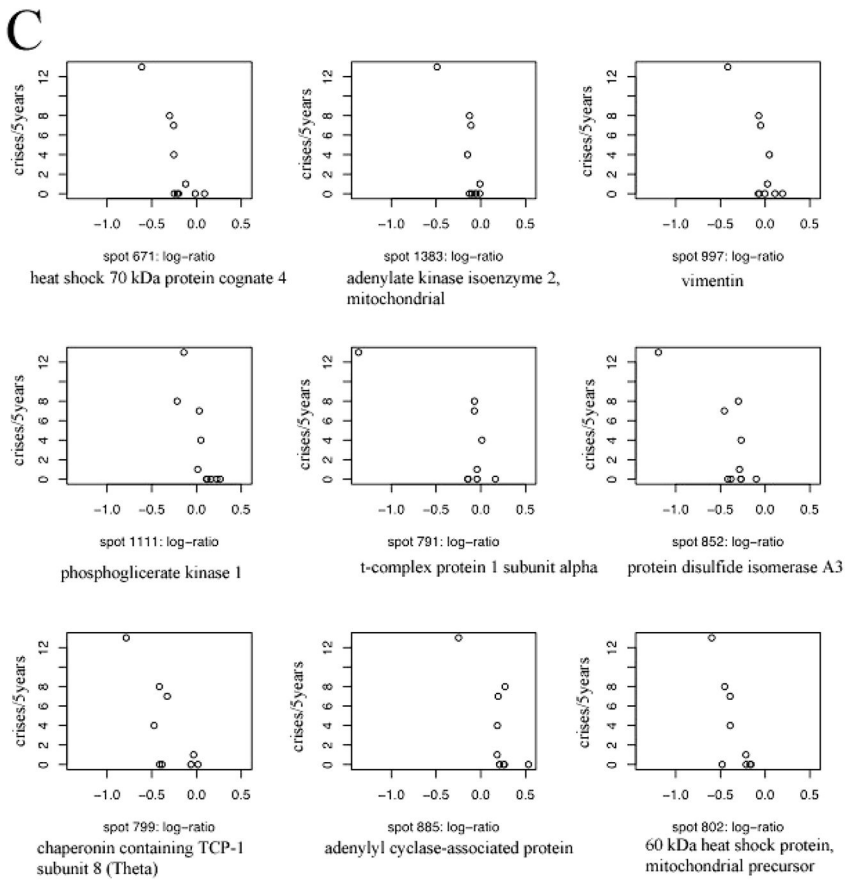


**Figure 2.**

Plots of crisis rate versus log-protein ratio. We present the 5-year number of vasoocclusive events (a measure of clinical severity) for the negatively correlated membrane fraction proteins (Panel A); and for positively (Panel B) and negatively (Panel C) correlated cytosolic fraction proteins that were successfully identified.

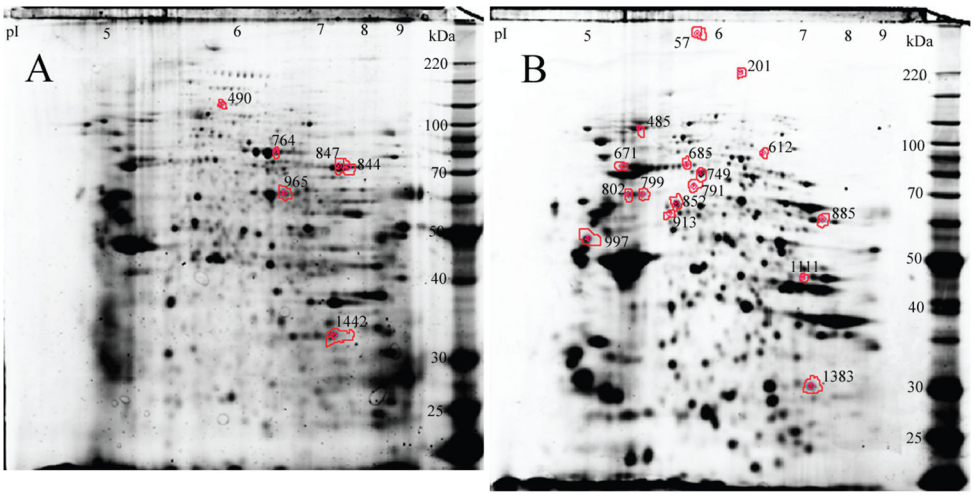


**Figure 3.**

Monocyte signatures of sickle cell crisis rate. Position of monocyte protein spots separated on a 2D IEF-SDS PAGE gel stained with Sypro Ruby that were successfully identified by tandem mass spectrometry. Monocyte proteins from the membrane fraction (Panel A) and cytosolic fraction (Panel B).

**Table 1**

Characteristics of the Patients and Quantitative Clinical Data

| Patient | Sex | Age (years) | Pain[1] (#) | ACS[1] (#) | Total[1] (#) | Hgb[2] (g/dL) | Retic[3] (%) | Hgb F[4] (%) | WBC[5] (/mm$^3$) |
|---|---|---|---|---|---|---|---|---|---|
| 1 | F | 15 | 0 | 0 | 0 | 7.5 | 12.4 | 5.3 | 15,500 |
| 2 | M | 17 | 1 | 2 | 3 | 7.0 | 18.5 | 19.9 | 9,500 |
| 3 | F | 14 | 8 | 0 | 8 | 9.3 | 10.1 | 8.3 | 11,100 |
| 4 | M | 16 | 0 | 0 | 0 | 8.2 | 16.9 | 10.0 | 11,200 |
| 5 | F | 13 | 4 | 0 | 4 | 7.3 | 15.7 | 19.1 | 9,900 |
| 6 | M | 18 | 0 | 0 | 0 | 9.1 | 8.9 | 13.8 | 18,000 |
| 7 | M | 18 | 0 | 0 | 0 | 8.0 | 11.1 | NA[6] | 11,100 |
| 8 | M | 14 | 0 | 2 | 2 | 7.5 | 18.3 | 5.1 | 10,300 |
| 9 | F | 16 | 7 | 0 | 7 | 9.0 | 9.3 | 3.5 | 10,500 |
| 10 | F | 18 | 13 | 3 | 16 | 8.6 | 10.4 | 13.1 | 9,600 |

[1] Number of vasoocclusive events in preceding 5 years.

[2] Steady-state hemoglobin concentration.

[3] Steady-state reticulocyte count.

[4] Porportion of fetal hemoglobin.

[5] Steady-state white blood cell (leukocyte) count.

[6] Not available.

**Table 2**

The Membrane Proteins that Are Most Negatively Correlated with Severity

| Spot number on 2D gel | MW(Da)/pI (experimental) | MW(Da)/pI (theoretical) | gi number | # of peptides | Protein ID |
|---|---|---|---|---|---|
| 844 | 74723/7.7 | 67877/7.58 | 4507521 | 4 | Transketolase |
| 847 | 74926/7.4 | 67878/7.58 | 4507521 | 4 | Transketolase |
| 965 | 62319/6.5 | 51026/6.25 | 5902134 | 3 | Coronin, actin binding protein |
| 764 | 81435/6.4 | 67820/6.08 | 4505257 | 3 | Moesin |
| 1442 | 32282/7.15 | 35076/7.6 | 5174447 | 4 | Guanine nucleotide binding protein, G protein |

**Table 3**

The Cytosolic Proteins that Are Most Positively Correlated with Severity

| Spot number on 2D gel | MW(Da)/pI (experimental) | MW(Da)/pI (theoretical) | gi number | # of peptides | Protein ID |
|---|---|---|---|---|---|
| 612 | 96342/6.5 | 73146/6.84 | 37078468 | 3 | Far upstream element-binding protein |
| 485 | 118057/5.4 | 103058/5.25<br>102268/5.27 | 4501891<br>2804273 | 5, 3 | Alpha actinin 1or alpha actinin 4 |
| 685 | 78342/5.7 | 66036/5.69 | 4389275 | 4 | Human serum albumin in a complex with myristic acid and tri-iodobenzoic acid |
| 57 | 272161/5.9 | 280739/5.7 | 116241365 | 3 | Filamin A |
| 201 | 168317/6.2 | 127177/6.76 | 64654539 | 4 | Integrin, alpha M |
| 913 | 63743/5.6 | 54445/5.69 | 28949044 | 3 | Chain A, Apo form of human mitochondrial aldehyde dehydrogenase |
| 749 | 82830/5.9 | 69285/5.8 | 4505029 | 9 | Leukotriene A-4 hydrolase |

*Exp Biol Med (Maywood)*. Author manuscript; available in PMC 2014 December 09.

**Table 4**

The Cytosolic Proteins that Are Most Negatively Correlated with Severity

| Spot number on 2D gel | MW(Da)/pI (experimental) | MW(Da)/pI (theoretical) | gi number | # of peptides | Protein ID |
|---|---|---|---|---|---|
| 671 | 87501/5.3 | 69285/5.8 | 12585261 | 5 | Heat shock 70 kDa protein cognate 4 |
| 1383 | 17024/7.6 | 14709/6.75 | 19526591 | 2 | Adenylate kinase 2 variant AK2D |
| 997 | 52648/4.9 | 53652/5.06 | 55977767 | 6 | Vimentin |
| 1111 | 46056/7.4 | 44603/8.3 | 48145549 | 4 | Phosphoglycerate kinase 1 |
| 791 | 72809/5.8 | 60344/5.8 | 57863257 | 7 | T-complex protein 1 subunit alpha |
| 852 | 66774/5.6 | 56782/5.98 | 2507461 | 3 | Protein disulfide-isomerase A3 [precursor] |
| 799 | 68814/5.4 | 59621/5.42 | 48762932 | 3 | Chaperonin containing TCP1, subunit 8 (theta) |
| 885 | 63966/8.0 | 51673/8.07 | 5453595 | 2 | Adenylyl cyclase-associated protein |
| 802 | 71428/5.3 | 61055/5.7 | 129379 | 3 | 60 kDa heat shock protein, mitochondrial precursor |